Wave Phenomena in Plasmas

Michael Schmid* and Henri Menke†
Gruppe M05, Fortgeschrittenenpraktikum, University of Stuttgart
(December 15, 2014)

In the present experiment we are going to measure different properties of waves in plasma. This is done using a *double plasma device*. First of all the dependency of the plasma starting on various parameters is observed. Next the plasma density is obtained using the plasma oscillation method. Using the aforementioned double plasma device we extract the dispersion relation of ion acoustic waves. Last and in contrast to the foregoing acoustic waves we study nonlinear shock waves in the plasma.

BASICS

In everyday life we experience matter in the three different phases: gaseous, liquid, and solid, albeit the fact that 99 % of visible matter in the universe resides in the plasma phase. *Plasma* is a gas, where gas particles are dissociated in electrons and ions. The concentration of both charged species is approximately equal. A plasma is neutral when viewed from the outside and can screen an inserted charge or applied fields; this is referred to as *quasi neutrality*.

Definition of Plasma

To qualify as a plasma an ionised gas has to fulfil certain properties:

1. The spacial extent of the plasma is much larger than the *Debye length*.
2. The particle density inside the *Debye sphere* is large.
3. The time between particle collisions is long compared to the cycle time of oscillations of the plasma with the plasma frequency.

Sometimes plasma is called the the “fourth phase”.

Plasma Parameters

Ionisation Condition

The *ionisation ratio* α is a proper quantity to decide whether there is a plasma. This is important, because plasma can be present at different pressures and temperatures. One has

$$\alpha = \frac{n_i}{n + n_i} \tag{1}$$

where n_i is the density of free charges and n is the total particle density.

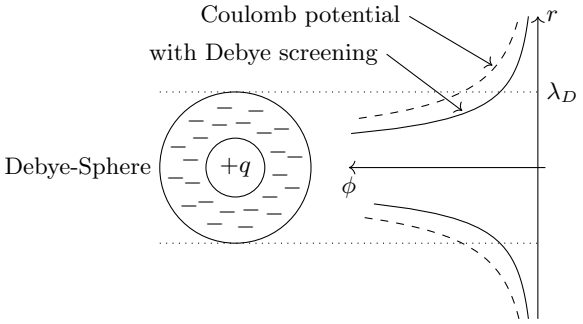

FIG. 1. A positive charge is screened by the plasma, i.e., the Coulomb potential decays faster. Based on [1, p. 8, fig. 1.3].

Debye Length

Inserted matter can be screened by a plasma through the presence of free charges. The insertion of a positive probe charge q_0 serves a good example. Negative charges aggregate around the probe charge, where aggregate is not good terminology, because the negative charges move with tremendous speed and solely their trajectories get a little deflected towards the probe charge. Nevertheless, a negative space-charge region is formed around the probe charge. The radius of this screen is called *Debye length* λ_D.

$$\lambda_D = \sqrt{\frac{\varepsilon_0 T}{e^2 n}} \approx 7.43 \cdot 10^3 \sqrt{\frac{T}{n}} \tag{2}$$

Here T is the (reduced) absolute temperature in eV and n is the particle density.

Debye Sphere

The aforementioned space-charge region does not grow to infinity, because further negative charges are repelled by the space-charge region. In exchange, positive charges are attracted and the screening of the probe charge is reduced. Consequently further negative charges get attracted to stabilise the screening. One might say, that there exist currents which either add or purge charges.

The Debye length is the radius of the Debye sphere. Obviously, a screening is only present if enough charges take part in it. The number of particles inside the Debye sphere is given by

$$N_D = n\frac{4}{3}\pi\lambda_D^3 = 1.72 \cdot 10^{12}\frac{T^{3/2}}{\sqrt{N}} \tag{3}$$

where n is the particle density and T is the temperature. To qualify as a plasma it must be that $N_D \gg 1$.

Quasi Neutrality

A probe charge inserted into the plasma is screened if the abundance of charges inside the Debye sphere equals the probe charge q_0. Because the plasma is neutral from the outside this is referred to as *quasi neutrality*. To fulfil this quasi neutrality two of the plasma criterions need to be met, viz. the particle density in the Debye sphere is large and the spacial extent of the plasma is huge compared to the Debye length. It is obvious why these have been employed here. Many particles are needed to form a screening double layer that does not leak and inside the debye sphere the plasma is not neutral, thus the plasma needs to be larger than the Debye length.

Plasma Frequency

To model a plasma in an electric field, one uses the *Lorenz-Drude model*. The force exerted on a particle in an electric field is given by

$$F_C = -eE. \tag{4}$$

From the Maxwell equations one has

$$\operatorname{div} \boldsymbol{E} = \frac{\varrho}{\varepsilon_0}. \tag{5}$$

If we assume the density $\varrho = e\, n_e$, one has in one dimension

$$m_e\ddot{x} = -e\frac{e\, n_e}{\varepsilon_0}x. \tag{6}$$

Solving this differential equation yields the so called *plasma frequency*. It is given by

$$\omega_P = \sqrt{\frac{e^2\, n_e}{\varepsilon_0\, m_e}}. \tag{7}$$

This means that the charge distribution inside the plasma cannot react faster to an external excitation than with the given frequency. Incident waves with $\omega < \omega_P$ thus get reflected by the plasma.

Waves in Plasma

In nature one may observe two kinds of propagating waves, viz. transversal and longitudinal. A typical example for a transversal wave are electromagnetic waves, whereas the longitudinal waves are well known as acoustic waves. We now focus on longitudinal waves in plasma. The main difference to transversal waves is that the displacement of the oscillating matter occurs in the direction of propagation. If a system described by the quantity A is perturbed by a plane wave one can find using perturbation theory

$$A = A_0 + A_1\, \mathrm{e}^{\mathrm{i}(\boldsymbol{kr}-\omega t)}. \tag{8}$$

The quantity A may be, e.g. an electric field or a density [1, p. 137].

Waves never propagate in perfect vacuum, that is why their intensity decreases over distance. The interaction with their wave support relaxes them towards zero, due to scattering at the particles of the support. Another possible mechanism is the Landau damping. Here it is assumed, that some particles of the longitudinal wave move much slower than the others. The slower particles absorb more energy from the waves, damping its velocity.

We know that transversal waves oscillate orthogonal to their direction of propagation, hence an electromagnetic wave with wave vector $\boldsymbol{k}$ fulfils the "modified Maxwell equations" [1, p. 138]. Suppose, there are waves propagating in the two-species plasma system (i.e. charges may be ions or electrons, denoted by indices i and e), then those equations read

$$\boldsymbol{k}\cdot\boldsymbol{B} = 0 \tag{9}$$

$$\mathrm{i}\varepsilon_0\boldsymbol{k}\cdot\boldsymbol{E} = \varrho_e + \varrho_i \tag{10}$$

$$\boldsymbol{k}\times\boldsymbol{E} = \omega\boldsymbol{B} \tag{11}$$

$$\mathrm{i}\boldsymbol{k}\times\boldsymbol{B} = \mu_0(\boldsymbol{j}_e + \boldsymbol{j}_i) - \mathrm{i}\frac{\omega}{c^2}\boldsymbol{E} \tag{12}$$

Using these equations it is feasible to derive the dispersion relation for longitudinal waves in the warm, demagnetised plasma [1, p. 153]

$$1 - \frac{\omega_{P,i}^2}{\omega^2 - c_i^2k^2} - \frac{\omega_{P,e}^2}{\omega^2 - c_e^2k^2} = 0, \tag{13}$$

where $\omega_{P,i}$ and $\omega_{P,e}$ is the plasma frequency of acoustic waves transported by ions and electrons, respectively.

The material-dependent propagation speed of the waves is given by c_i and c_e (in case of acoustic waves this is equivalent to the speed of sound). If $\omega^2 > c_e^2k^2 \gg c_i^2k^2$ the above equation has no singularities and we may neglect the plasma frequency of the ions c_i as tiny compared to the electrons. We also neglect 1 and obtain [1, p. 155]

$$\omega_{P,e}^2(\omega^2 - c_i^2k^2) = \omega_{P,i}^2c_e^2k^2. \tag{14}$$

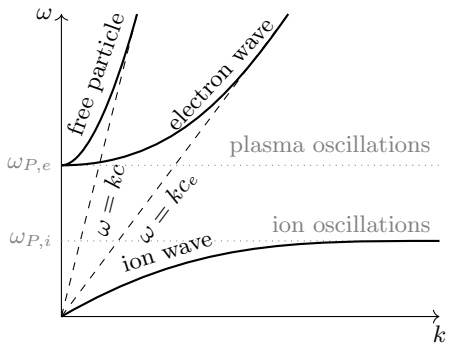

FIG. 2. Dispersion relation for longtidunual waves in the warm, demagnetised plasma, freely adapted from [1, fig. 5.12].

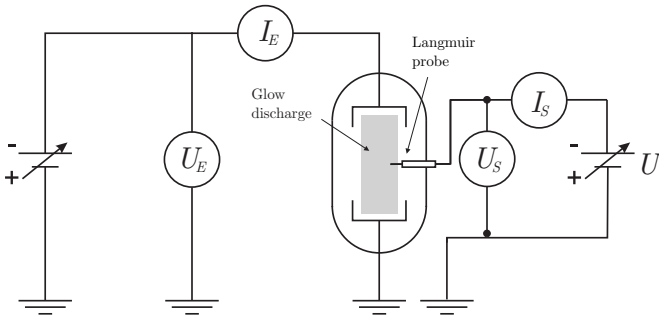

FIG. 3. Circuit diagram for a glow discharge using a Langmuir probe, from [2, p. 2].

Plugging in the definition of the species temperature one has

$$\omega = \sqrt{\frac{T_e + 3T_i}{m_i}}k. \tag{15}$$

Langmuir Probes

An often used device for diagnostics of plasma parameters is the so called *Langmuir probe*, named after its developer Irving Langmuir. It consists of a simple electrode which is inserted into the plasma. At equal ion and electron temperature, electrons have a much greater mobility than the ions and thus hit the surface of the probe much more often, where they induce a negative space-charge. As an equilibrium of ion and electron current arrives, the potential that arises then between the probe and the ground is called *floating potential* Φ_{fl}.

If the probe is set to a negative potential before insertion, the electrons get repelled while the ions are attracted. For voltages large enough all ions from the surrounding plasma get evacuated and a saturation current settles to

$$I_{i,\text{sat}} = 0.61\, enS\sqrt{\frac{T_e}{m_e}}. \tag{16}$$

For further increasing voltages only electrons with sufficient thermal energy can reach the probe surface. The

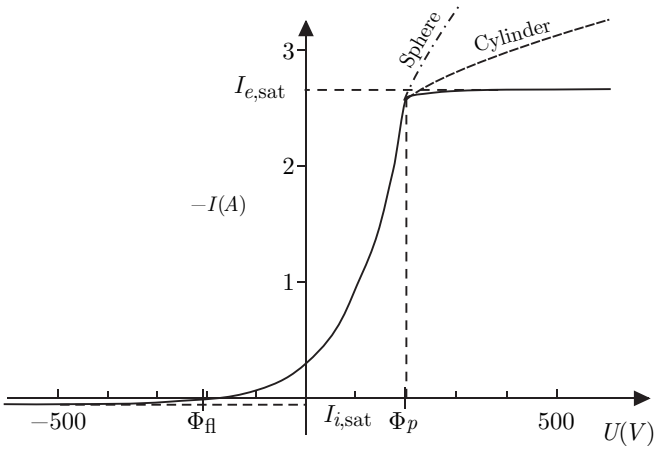

FIG. 4. Characteristic curve of a Langmuir probe, from [2, p. 2].

root of the characteristic curve of the Langmuir probe is at $\Phi = \Phi_{\text{fl}}$, the range where electrons can reach the surface ends at the plasma potential $\Phi = \Phi_p$. In the range where electrons can reach the surface the characteristic curve is given by

$$I_e = I_{e,\text{sat}} \exp\left(-\frac{e(\Phi_p - U)}{T_e}\right) \tag{17}$$

with

$$I_{e,\text{sat}} = -enS\sqrt{\frac{T_e}{2\pi m_e}}. \tag{18}$$

A sample graph of the characteristic curve is given in figure 4.

The complete measurable current at the probe in the range where electrons can reach the surface is the sum of ion saturation current and electron current, viz.

$$I = I_i + I_e = I_{e,\text{sat}} \exp\left(-\frac{e(\Phi_p - U)}{T_e}\right) + I_{i,\text{sat}}. \tag{19}$$

Some simple conversions yield

$$\ln\Big(I_{i,\text{sat}} + I_e\Big) = \ln\Big(-I_{e,\text{sat}}\Big) - \frac{e(\Phi_p - U)}{T_e}. \tag{20}$$

With these formulas we can conclude the plasma parameters from the characteristic curve. With the knowledge of the gas temperature and the gas pressure also the electron temperature and the electron density can be computed.

Double Plasma Device

For the measurement of waves in the plasma we are going to use the *double plasma device*, which is described thoroughly in [3]. A sketch of such a double plasma device setup is shown in figure 5.

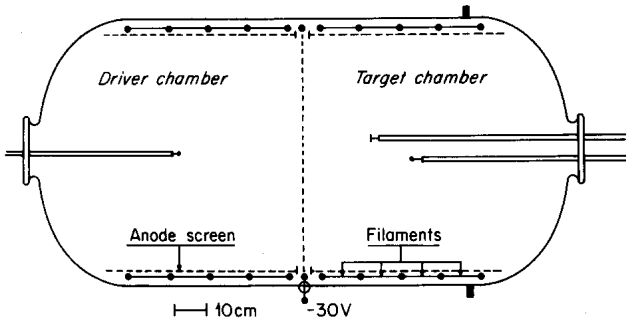

FIG. 5. A common double plasma device, taken from [3]. One can see the two vacuum chambers with the inserted filaments and the separating grid.

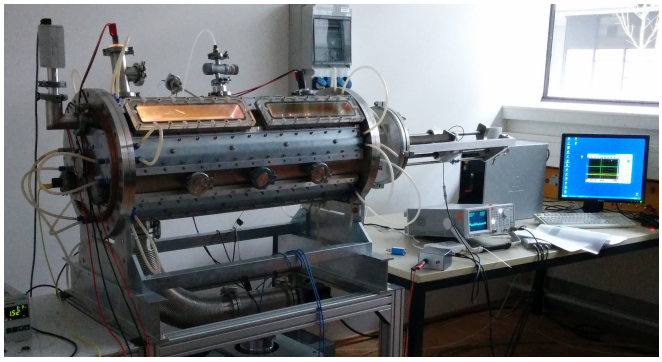

FIG. 6. Photo of the experimental setup. The huge metal cylinder is the double plasma device we used to investigate wave phenomena in plasma.

The apparatus consists of two vacuum chambers, each of them able to contain a plasma, separated by a negatively biased grid which is thus only permeable for ions. Filaments are inserted in each chamber to give rise to a plasma by applying a discharge voltage U_D. As depcited, there is an additional anode screen placed in the source chamber (driver chamber in the figure). The additional "stick" in the target chamber is a moveable Langmuir probe to conduct measurements of the ion acoustic waves. Because the chambers are evacuated there is a pressure control, which obviously influences the particle density inside.

Before, we mentioned the grid, separating the two chambers, which is set to a negative potential. This grid operates as a coupling between the two chambers. Due to the negative potential electrons are repelled. This allows for the excitation of ion acoustic waves which can pass (nearly) without interaction through the grid. Detection of those waves is performed by the Langmuir probe.

ANALYSIS

In this section we discuss the experimental procedures and the analysis of the measured data.

Experimental Tasks and setup

The experiment is mainly divides in four experimental tasks.

Discharge Current: After starting the plasma we measure the discharge current $I_{S,\text{source}}$. To investigate the behaviour of $I_{D,\text{source}}$ as function of the discharge voltage $U_{D,\text{source}}$, the heating current $I_{H,\text{source}}$, and the neutral gas pressure p we conduct several measurements. To investigate the dependency on one of the aforementioned quantities we hold the other two constant. We repeat these measurements with the filament switched on in the target chamber.

Plasma Oscillation Method: With help of the plasma oscillation method it is possible to determine the density of the plasma. Therefore we excite the oscillations at the plasma frequency with an electron beam where we set $U_{D,\text{source}} \approx 100\,\text{V}$. Note that the beam density should be low during the experiment. The axially movable Langmuir probe allows for the measurement of the oscillations. To do so we analyse the measured signal with a spectrum analyser. Then we repeat the measurements as described above.

Ion Acoustic Waves: To investigate the dispersion relation and the damping of the ion acoustic waves with the Langmuir probe we first have to excite the ion acoustic waves by applying a sinusoidal voltage to the grid. The measured spectra are analysed with a computer. Therefore we start at a maximum of the amplitude and move the Langmuir probe to the next adjacent maximum. The measured amplitude over the distance allows us to determine the spatial damping. Three measurements of the dispersion relation and the spatial damping are performed for different gas pressures p.

Nonlinear Shock Waves: By raising the amplitude of the sinusoidal voltage it is possible to investigate the regime of nonlinear effects. The appearing nonlinearities are recorded with an oscilloscope.

The experimental setup is depicted in figure 6. The plasma is generated in a cylindrical double plasma device which contains two filaments to ignite the plasma. With help of a computer and a spectrum analyser on the right side of the figure it is possible to analyse and measure the desired quantities. The long stick on the right side of the plasma device is the only visible part of the Langmuir probe. The probe itself is incorporated in the plasma device and thus not visible.

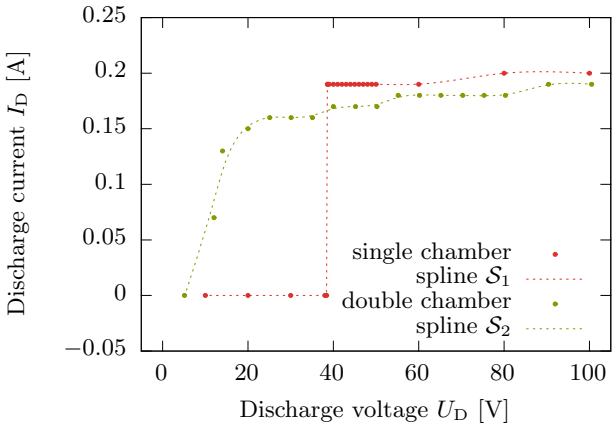

FIG. 7. Measurements of the discharge current I_D of the source chamber over the discharge voltage U_D. The measured data belonging to the measurement with just one switched on filament (source chamber) is coloured red. Accordingly the green data points belong to a measurement with both filaments switched on. For better visibility two splines with the corresponding colours are plotted alongside.

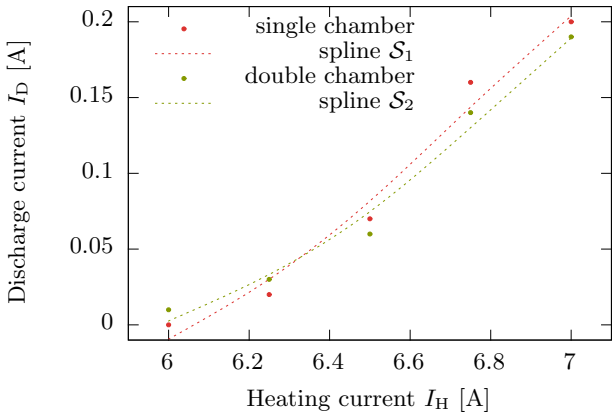

FIG. 8. Measurements of the discharge current I_D of the source chamber over the heating current I_H. The measured data belonging to the measurement with just one switched on filament (source chamber) is coloured red. Accordingly the green data points belong to a measurement with both filaments switched on. For better visibility two splines with the corresponding colours are plotted alongside.

Dependency of the Discharge Current

To perform any measurements we first need to start the plasma in the vacuum chambers. This is done by heating the filaments and applying a discharge voltage to them. The transition to the plasma phase is indicated by the discharge current which is then $\neq 0$. A stable plasma was obtained for a heating voltage of $U_{H,\text{source}} = 10.02\,\text{V}$, a heating current of $I_{H,\text{source}} = 6.859\,\text{A}$ and a gas pressure of $p = 3.08\,\text{mPa}$. With these parameters at hand the dependency of the discharge current on the following parameters was studied: the discharge voltage, the heating current and the gas pressure.

Discharge Voltage: Holding all parameters constant and varying the discharge voltage in a range from 5 V to 100 V we noted down the discharge current of the source chamber. This was done for the case of a turned on filament in the source chamber and the case of both turned on filaments. The corresponding data is depicted in figure 7. For the case of the single chamber (red data points) we observed a jump from 0.0 A to 0.19 A for a discharge voltage near 38.5 V. For higher voltages the measured discharge current remains nearly constant. In case of the measurements with both chambers (green data points) the jump is not observed. The two measurements yield a saturation current from 0.18 V to 0.2 V. The plateau of saturation appears due to the increasing negative space-charge region for increasing U_D around the filaments. Electrons emitted from the filament therefore need a higher energy to overcome this region. Working with both chambers is therefore more suitable to investigate the properties of plasma.

Heating Current: Varying now the heating current of the source chamber leads to the measured data shown in figure 8. Except for some small deviations the measured data in case of the single chamber measurement and the double chamber measurement show the same behaviour of the discharge current as a function of the heating current. Hence it seems that there is no dependency of the heating current on a switched on or off target chamber filament. The depicted splines $\mathcal{S}_1$ and $\mathcal{S}_2$ for the corresponding measured data show an increasing slope for increasing heating current. Obviously this is due to the higher emitting rate of electrons of the filaments for higher heating currents.

Gas pressure: The parameter varied last is the gas pressure p. In figure 9 the measured data for both measurement cases is depicted. For both cases we observe an increasing discharge current of the source chamber for increasing gas pressure.

Plasma Oscillation Method

To measure the plasma density we use the plasma oscillation method. The electrons emitted by the filaments of the target chamber excite oscillation at the plasma frequency. To hold the beam density low we set the discharge voltage $U_{D,\text{target}} = 100\,\text{V}$ to achieve a low discharge current of the target chamber, where we measured $I_{D,\text{target}} = 0.08\,\text{A}$. The other parameters were set to $U_{H,\text{source}} = 11.21\,\text{V}$, $p = 4.54\,\text{mPa}$ and $I_{H,\text{source}} = 7.207\,\text{A}$. For the subsequent measurements we can therefore neglect $I_{D,\text{target}}$. The oscillations were detected with an axial Langmuir probe. The measured

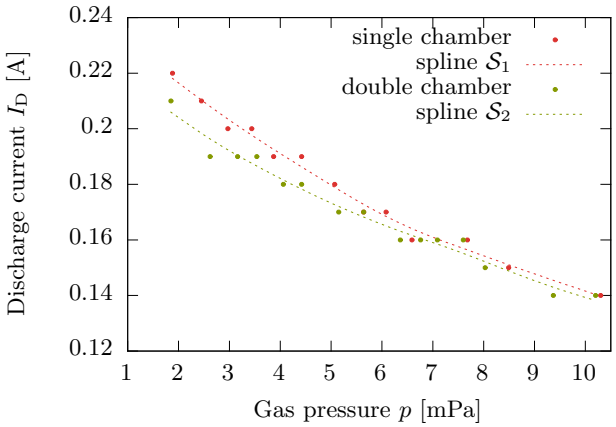

FIG. 9. Measurements of the discharge current I_D of the source chamber over gas pressure p in the whole double plasma device. The measured data belonging to the measurement with just one switched on filament (source chamber) is coloured red. Accordingly the green data points belong to a measurement with both filaments switched on. For better visibility two splines with the corresponding colours are plotted alongside.

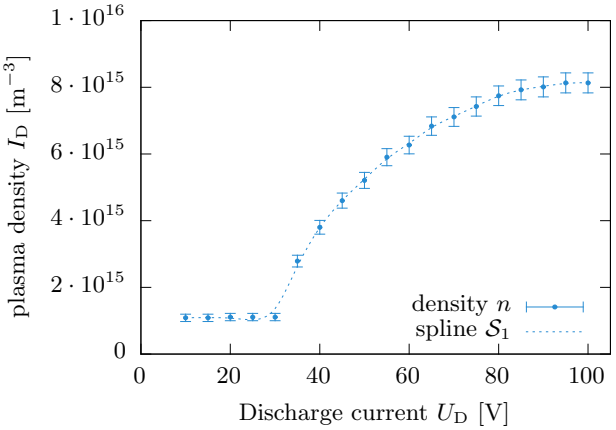

FIG. 10. Plasma density n as a function of the discharge voltage U_D of the source chamber. During the measurement the different parameters were held constant. For better visibility the data is overlayed with a spline.

signal is then analysed with help of a spectrum analyser. To do so we first had to spot the right peak in the spectrum analyser for the plasma frequency. Varying some of the parameters caused a shifting of the peak belonging to the plasma frequency. Note that the spectrum analyser measures only frequencies ν and not angular frequencies ω. Next we measured the plasma freuquency as a function of different parameters, viz. the discharge voltage $U_{D,\text{source}}$, the heating current $I_{H,\text{source}}$, and the gas pressure p. With help of the formula

$$\omega_p = 56.5\,\sqrt{n}, \tag{21}$$

from [1] it is possible to determine the plasma density n. A simple conversion yields

$$n = \left(\frac{\omega_p}{56.5}\right)^2. \tag{22}$$

Discharge Voltage: At first we measured the plasma frequency as a function of the discharge voltage of the source chamber. Therefore we measured the plasma frequency with the spectrum analyser while varying the voltage from 10 V to 100 V in steps of 5 V. With help of equation (22) we determined the plasma density depicted in figure 10. For sufficiently high voltages (higher than 30 V) the plasma density increases. For low voltages it is nearly constant. Obviously this is due to the higher kinetic energy of the emitted electrons for higher discharge voltages. For high voltages the plasma density seems to saturate to a constant value.

Heating Current: The plasma density as function of the heating current $I_{H,\text{source}}$ is depicted in figure 11. Only for sufficiently high heating currents we observed an increasing plasma density. For currents lower than 6.5 A

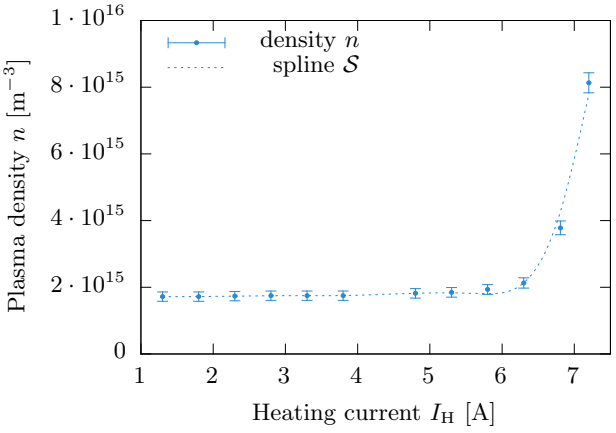

FIG. 11. Plasma density n as a function of the heating current of the source chamber $I_{H,\text{source}}$. The figure shows that only for sufficiently high heating currents the plasma density increases in a significant manner. For the lower heating currents it remains nearly constant.

the plasma density remains constant. The measurement corresponds with our expectations, because for higher heating currents more emitted photons are able to ionise gas particles.

Gas Pressure: The plasma density n as function of the gas pressure p is depicted in figure 12. Like in the previously discussed cases the curve seems to saturate for high gas pressure. An additionally plotted spline $\mathcal{S}$ emphasises the increasing character for increasing pressures.

Note that we assumed for all plotted data an error of $\Delta\nu = 7.5\,\text{MHz}$. The noisy spectrum of the spectrum analyser corresponds with this error for the frequency.

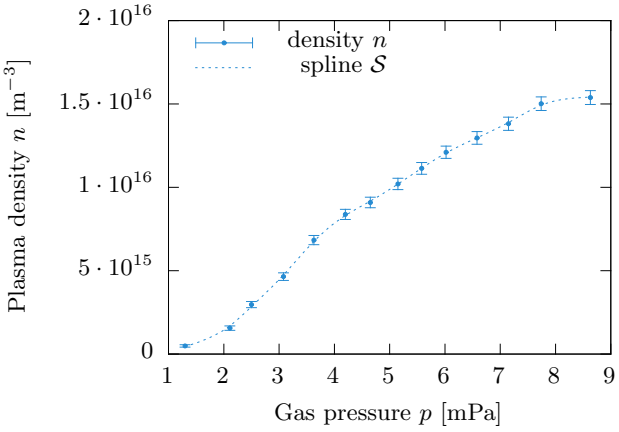

FIG. 12. Plasma density n as a function of the gas pressure p in the whole two chamber device. Obviously the plasma frequency depends on the gas pressure. For better visibility a spline is also plotted.

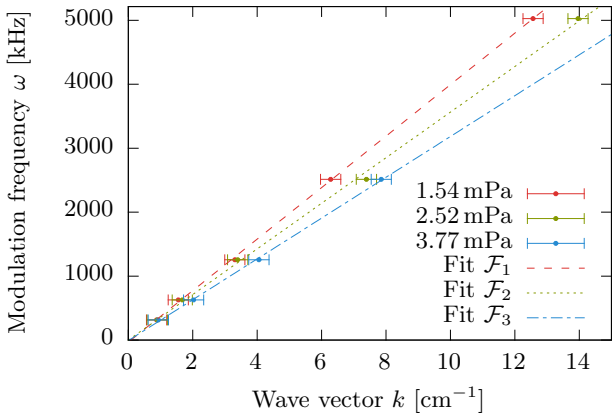

FIG. 13. Modulation frequency ω as a function of the wave vector k. For three different pressures the data is fitted with a linear function $\mathcal{F}_i$ where $i \in \{1, 2, 3\}$. With the slope of the fit it is possible to determine the speed of sound.

Ion Acoustic Waves

Applying a sinusoidal voltage to the grid and using the Langmuir probe allows us to measure the dispersion relation for three different gas pressures and the damping length λ. Because the measured data is very noisy we assumed an error for the amplitude of the signal of $\Delta A = 15\,\mathrm{mV}$ and for the measured frequencies an error of $\Delta\nu = 7.5\,\mathrm{MHz}$.

Dispersion Relation: For ion acoustic waves we expect a linear dispersion relation

$$\omega(k) = \sqrt{\frac{T_e + 3T_i}{m_i}}k = c_s k, \tag{23}$$

where T_e is the temperature of the electrons, T_i the temperature of the ions, m_i the mass of the Ar ions, and c_s the speed of sound. To determine c_s from the measured data, depicted in figure 13, we fitted a linear function

$$\mathcal{F}_i(x) = a_i x + b_i \tag{24}$$

where i indicates the three measurements for different gas pressures. Obviously only a_i gives us the speed of sound. The fit gives us the three parameters

$$a_1 = 4025.52\,\mathrm{m\,s^{-1}}, \tag{25}$$
$$a_2 = 3564.53\,\mathrm{m\,s^{-1}}, \tag{26}$$
$$a_3 = 3191.09\,\mathrm{m\,s^{-1}}. \tag{27}$$

Taking the average value yields the speed of sound

$$\bar{c}_s = 3593.71\,\mathrm{m\,s^{-1}} \tag{28}$$

To calculate the temperature of the electrons T_e we have to keep in mind, that $T_e \gg T_i$ and can therefore neglect T_i in the subsequent analysis. Using equation (23) leads to

$$T_e = m_i \bar{c}_s^2 \tag{29}$$
$$= 5.348\,\mathrm{eV}. \tag{30}$$

This corresponds to a "real" temperature $T = T_e/k_\mathrm{B} = 6.205 \cdot 10^4\,\mathrm{K}$.

Damping: To investigate the damping we measured the data for a pressure of $p = 7.09\,\mathrm{Pa}$ and used a fit of the form

$$\mathcal{F}(x) = A\mathrm{e}^{-\frac{x}{\lambda}} \tag{31}$$

where λ is the damping length and A the amplitude. In a semi-logarithmic plot this corresponds with a simple line as shown in figure 14. The depicted fit function possesses the parameters

$$A = 336.08\,\mathrm{mV}, \tag{32}$$
$$\lambda = 11.527\,\mathrm{cm}, \tag{33}$$

which show an exponential decay.

Nonlinear Shock Waves

To investigate the transition from the linear ion acoustic waves to nonlinear shock waves it is necessary to amplify the sinusoidal voltage. The observed changes in the signal are depicted in figure 15 and 16.

First we amplified a rectangle signal as shown in figure 15. The higher the amplifying factor Γ the better the transition is visible and the signal gets deformed. In case of a sinusoidal signal as depicted in figure 16 the same behaviour of the signal is visible. As described in [4] it is then possible to determine the plasma frequency ω_pi. To

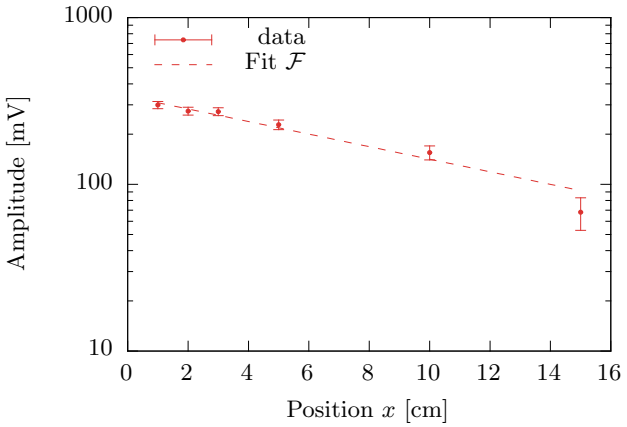

FIG. 14. Semi-logarithmic plot for the amplitude of the measured signal as a function of the position x of the Langmuir probe in the double chamber device. From the exponential fit $\mathcal{F}$ it is possible to obtain information about the damping length.

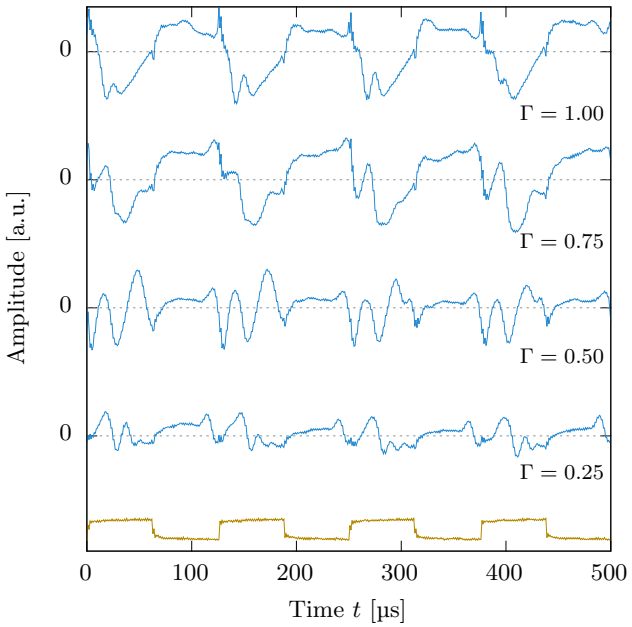

FIG. 15. Signal of the Langmuir probe as recorded by an oscilloscope. The signal form which is applied to the grid is a rectangle (yellow). One can see, that for increasing modulation amplitude of the voltage in the grid, the curves get deformed.

do so we have to measure the time distance between two adjacent extrema. This yields

$$\omega_{\mathrm{pi}} \approx 48.3\,\mathrm{kHz}. \tag{34}$$

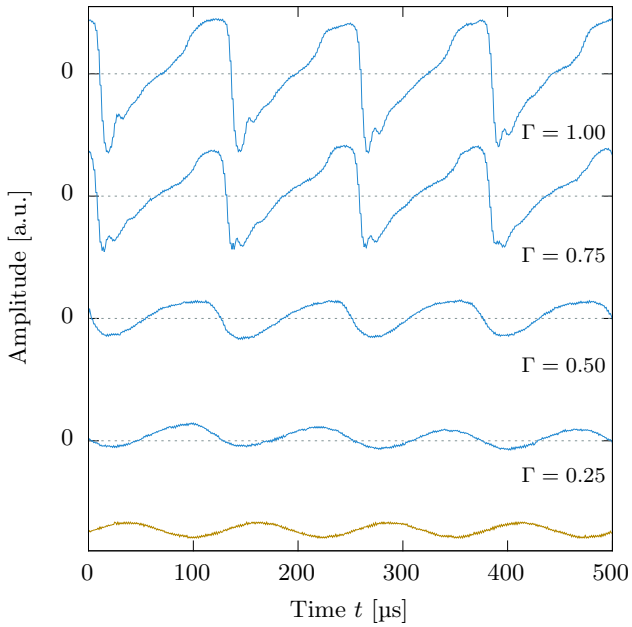

FIG. 16. Signal of the Langmuir probe as recorded by an oscilloscope. The signal form which is applied to the grid is a sine (yellow). One can see, that for increasing modulation amplitude of the voltage in the grid, the curves get deformed.

Error Discussion

To analyse the measured data we used errors in the amplitude, measured frequency and the wave vector as described in the section above. This was necessary because the observed signals on the computer or the spectrum analyser were very noisy.

SUMMARY

Dependency of the Discharge Current: The dependency on the discharge voltage turned out to have the weird property of jumping from zero to a plateau of constant discharge current. This could be rectified though by enabling the discharge through the target chamber filament as well. The overall course is then smooth but the saturation towards a plateau persists.

For varying heating current no serious differences were present between the single chamber and double chamber setup. The discharge current exhibits an increasing slope which could be an exponential.

This case seems to be exactly inverted when modifying the gas pressure. The discharge current is decreasing with increasing pressure just like an exponential decay.

Plasma Density: The plasma oscillation method was applied to extract the plasma density. The dependency on the same parameters as in the previous task was studied. For increasing discharge current we again reach a

plateau, for increasing heating current we find a divergent behaviour, while for the gas pressure the plasma density seems to increase linearly.

Ion Acoustic Waves: Using the Langmuir probe the dispersion relation was recorded for three different gas pressures. The resulting curves were fitted with a linear function to extract their slopes. These slopes correspond to the speed of sound. To get a better approximation all values were averaged and one has

$$\bar{c}_s = 3593.71\,\mathrm{m\,s^{-1}}. \tag{35}$$

From this we can compute the electron temperature

$$T_e = 5.348\,\mathrm{eV} \mathrel{\hat{=}} 6.205 \cdot 10^4\,\mathrm{K}. \tag{36}$$

The exponential decay of the amplitude for increasing distance to the source of the waves yields a damping length of

$$\lambda = 11.527\,\mathrm{cm}. \tag{37}$$

Nonlinear Shock Waves: Increasing the amplitude of the modulation signal on the grid transfers the waves to a regime of nonlinear shock waves. From the recorded spectra we extracted the plasma frequency

$$\omega_{\mathrm{pi}} = 48.3\,\mathrm{kHz} \tag{38}$$

* Michael_1233@gmx.de
† henrimenke@gmail.com

[1] U. Stroth, *Plasmaphysik: Phänomene, Grundlagen, Anwendungen*, Studium (Vieweg+Teubner Verlag, 2011).
[2] S. Merli, *Elektrische Sonden im Plasma* (2013).
[3] R. J. Taylor, K. R. MacKenzie, and H. Ikezi, Review of Scientific Instruments **43**, 1675 (1972).
[4] R. Taylor, D. Baker, and H. Ikezi, Physical Review Letters **24**, 206 (1970).
[5] K. Rumiantcev, *Wave phenomena in plasmas* (2014).